ChemPubSoc Europe
DOI: 10.1002/slct.201600351
Chemistry SELECT Communications

Catalysis

Realizing Selective and Aerobic Oxidation by Porous Transition-Metal-Salt@Ceria Catalyst

Pengfei Zhang,*[a] Hanfeng Lu,[e] Shize Yang,[c] Wangcheng Zhan,[a] Wenshuai Zhu,[a] Xueguang Jiang,[b] Caili Huang,[d] and Sheng Dai*[a, b]

In the past decades, ceria-based materials have been well developed as catalysts for complete oxidation; however, only a very few studies have involved ceria-promoted selective oxidations. Herein, porous transition-metal-salt–doped ceria (TMS@CeO_2) materials (up to 455 m^2/g) were fabricated by a simple, general co-assembly strategy with ionic liquids as recyclable templates. The TMS@CeO_2 catalyst was found to be active in the selective oxidation of sulfides to sulfoxides/sulfones by molecular oxygen. It is interesting that the TMS doping significantly increases the catalytic performance of the original ceria catalyst and, surprisingly, the TMS@CeO_2 catalyst showed much higher activity than a transition metal–doped cerium oxide solid solution. The TMS and CeO_2 are supposed to synergistically activate O_2 at the interface. It is believed that the abundant ceria-based materials will provide more efficient catalysts for controlled oxidation in the near future.

Ceria is one of the most attractive candidates toward catalytic oxidation because of its excellent redox property, good oxygen storage and release capacity, and accessible high surface area.[1] In past decades, ceria or doped-ceria materials have been found to be active in catalytic wet oxidation of pollutants in wastewater and in total oxidation of volatile organic compounds, hydrocarbons, CO, and other emissions.[2] However, almost all of the oxidation processes promoted by ceria-based materials focus on complete oxidation with CO_2 and/or H_2O as products. Therefore, the interesting question remains whether ceria-based catalysts can promote selective oxidation—one of the most frequently used processes in the manufacture of bulk and fine chemicals.[3] This hypothesis becomes possible if desorption of the substrate from reactive catalyst surface can occur before a complete decomposition. It is understandable that performing catalytic oxidation with ceria-based materials at a low temperature (e.g., $<150^\circ C$) may preserve the oxidized intermediates or products.[4] Just recently, Tamura *et al.* showed ceria-mediated imine formation (including oxidative dehydrogenation of benzyl alcohol to benzaldehyde) at 303 K, suggesting that the redox property of ceria at a low temperature may function for selective oxidation.[5]

In this contribution, we show a family of highly porous transition-metal-salt–doped ceria catalysts (TMS@CeO_2, up to 455 m^2g^{-1}) with moderate to good performances in the selective oxidation of sulfides to sulfoxide/sulfones by molecular oxygen. The current strategy for directing porosity into TMS@CeO_2 is actually solvent-evaporation–induced assembly of TMS and cerium precursors around ionic liquid (IL) clusters/aggregations.[6] During the slow hydrolysis (50°C) of cerium 2-methoxyethoxide, metal salts (e.g., $Mn(OAc)_2$, $Mn(acac)_2$, $Fe(OAc)_2$, $Co(OAc)_2$, $Ni(OAc)_2$, or $Cu(OAc)_2$) are evenly incorporated into the ceria backbone, followed by aging of the composite film at 200°C (Scheme 1). Finally, ILs are recovered by refluxing the composite in ethanol; at that time, rich porosity is released. The samples are labelled as "10%$Mn(OAc)_2$@CeO_2," *etc.*, where "10%" refers to the molar ratio of manganese. This process is different from the IL-mediated synthesis of metal oxides/per-

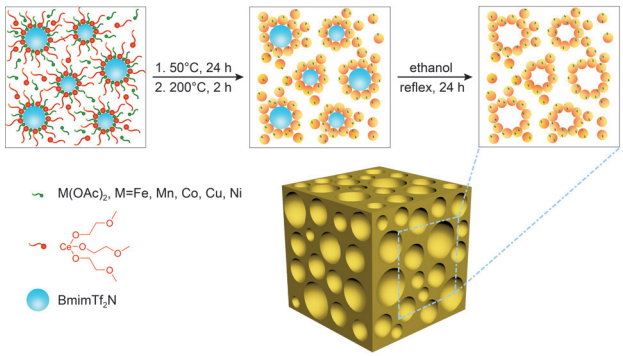

Scheme 1. A simple strategy for construction of porous transition-metal-salt@CeO_2 materials.

[a] *Dr. P. Zhang, Dr. W. Zhan, Dr. W. Zhu, Prof.Dr. S. Dai*
Chemical Sciences Division
Oak Ridge National Laboratory, Oak Ridge, TN 37830, USA
E-mail: chemistryzpf@163.com
dais@ornl.gov
[b] *Dr. X. Jiang, Prof.Dr. S. Dai*
Department of Chemistry
University of Tennessee
Knoxville 37996, TN, USA
[c] *Dr. S. Yang*
Materials Science and Technology Division
Oak Ridge National Laboratory, USA
[d] *Dr. C. Huang*
Neutron Science Directorate
Oak Ridge National Laboratory, USA
[e] *Dr. H. Lu*
Institute of Catalytic Reaction Engineering, College of Chemical Engineering, Zhejiang University of Technology, Hangzhou 310014, China

Supporting information for this article is available on the WWW under http://dx.doi.org/10.1002/slct.201600351

ovskites/metal nitride, in which calcinations at high temperatures (e.g., 500–700°C) are used for the formation of crystalline composites.[7]

The presence of acetate ions in 50%Mn(OAc)$_2$@CeO$_2$ was suggested by Fourier transform infrared spectroscopy (FTIR) peaks at ~1525 cm^{-1} and ~1398 cm^{-1}, corresponding to the vibration sorption of acetate ions (Figure 1**a, Figure S1**). These

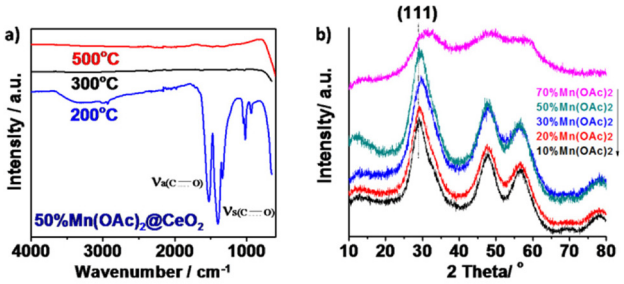

Figure 1. (a) FTIR spectra of 50%Mn(OAc)$_2$@CeO$_2$ samples at different temperatures. (b) XRD patterns of Mn(OAc)$_2$@CeO$_2$ samples with different doping amounts..

peaks disappeared after thermal treatment of the sample at 300°C, during which the Mn(OAc)$_2$ may decompose into oxide (decomposition temperature: ~275°C). X-ray diffraction (XRD) patterns of the Mn(OAc)$_2$@CeO$_2$ samples confirmed the successful formation of a cubic fluorite structure; meanwhile the broad diffraction peaks for the (111) planes revealed the small average crystalline size of Mn(OAc)$_2$@CeO$_2$ (~1.3 nm by the Scherrer equation for 50%Mn(OAc)$_2$@CeO$_2$, Figure 1**b**). Therefore, 200°C proved to be a suitable temperature that can guarantee the preservation of metal acetate salts and at the same time enable the formation of crystalline ceria.

The porosity of TMS@CeO$_2$ was investigated by N$_2$ sorption measurement at 77 K. The isotherm curves of doped ceria with low Mn(OAc)$_2$ amounts (10, 20, and 30 mol%,) were type IV/H2 sorption profiles with capillary condensation features at P/P$_0$ ≈0.5—characteristics of mesoporous materials, in agreement with the pore size distributions, which were located between 2 and 12 nm (Figure 2**a, Figure S2**). At high Mn(OAc)$_2$ doping amounts, the pore size moved toward the microporous domain. The 50%Mn(OAc)$_2$@CeO$_2$ sample afforded a high specific surface area of 455 m^{2}g^{-1}, higher than the value for a CeO$_2$ sample (192 m^{2}g^{-1}) (Table 1). The ceria samples doped with other metal salts, such as 50%Fe(OAc)$_2$@CeO$_2$, 50%Co(OAc)$_2$@CeO$_2$, 50%Ni(OAc)$_2$@CeO$_2$, and 50%Cu(OAc)$_2$@CeO$_2$, showed high N$_2$ uptake at low relative pressures (<0.1) with a plateau between $0.1 < P/P_0 < 0.9$; and the type I sorption behaviour suggested that the porosity was dominated by micropores (Figure 2**b**). The corresponding specific surface areas were 186–234 m^{2}g^{-1}. Ternary ceria-based materials, including two different TMSs, also could be fabricated. The 20%Fe-30%Mn(OAc)$_2$@CeO$_2$ and 20%Cu-30%Mn(OAc)$_2$@CeO$_2$ samples possessed hierarchically porous structures with specific surface areas of 376 and 344 m^{2}g^{-1}, respectively. Hence, it is fair to say

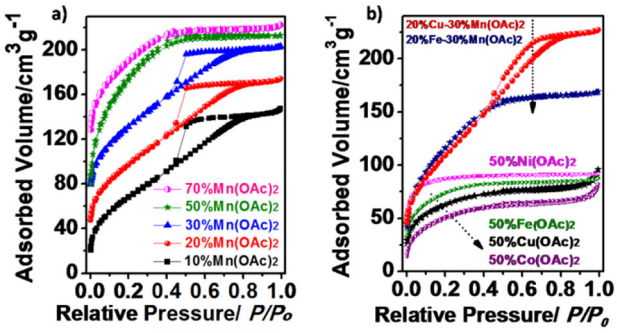

Figure 2. (a) 77 K N$_2$ sorption isotherms of Mn(OAc)$_2$@CeO$_2$ samples with different doping amounts; for clarity, the isotherm curves were offset by 30 cm^3/g for 20%Mn(OAc)$_2$@CeO$_2$, 60 cm^3 for 30%Mn(OAc)$_2$@CeO$_2$, 50 cm^3 for 50%Mn(OAc)$_2$@CeO$_2$, and 110 cm^3 for 70%Mn(OAc)$_2$@CeO$_2$. (b) 77 K N$_2$ sorption isotherms of doped CeO$_2$ samples with different transition metal salts; for clarity, the isotherm curves were offset by 10 cm^3/g for 50%Cu(OAc)$_2$@CeO$_2$ and by 20 cm^3/g for 50%Fe(OAc)$_2$@CeO$_2$, 50%Ni(OAc)$_2$@CeO$_2$, 20%Fe-30%Mn(OAc)$_2$@CeO$_2$, and 20%Cu-30%Mn(OAc)$_2$@CeO$_2$.

that IL-mediated co-assembly is a general strategy for directing porosity into TMS@CeO$_2$.

The porous morphology of TMS@CeO$_2$ was directly witnessed by transmission electron microscopy (TEM) and scanning TEM-high angle angular dark field (STEM-HAADF) images (Figure 3 **and Figure S3**). Abundant porosities with apparent

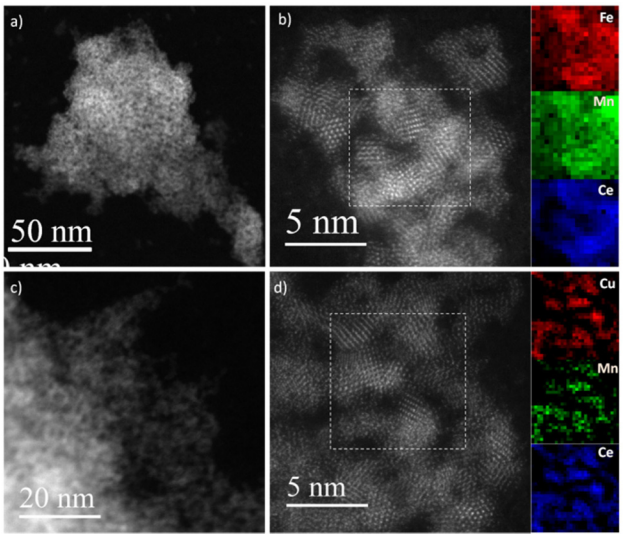

Figure 3. (a) and (b) STEM-HAADF images of 20%Fe-30%Mn(OAc)$_2$@CeO$_2$ with EELS; (c) and (d) STEM-HAADF images of 20%Cu-30%Mn(OAc)$_2$@CeO$_2$ with EELS.

pores within the microporous and mesoporous domains were observed in the TMS@CeO$_2$ samples, in accordance with the results of N$_2$ sorption measurements. The removal of large IL clusters/aggregations was considered to lead to the porous matrix, similar to the ionothermal synthesis of porous carbon materials. (Figures 3a, 3c, S3).[8] Actually, the TMS@CeO$_2$ samples were

Table 1. Aerobic oxidation of methyl phenyl sulfide by ceria-based catalysts[a]

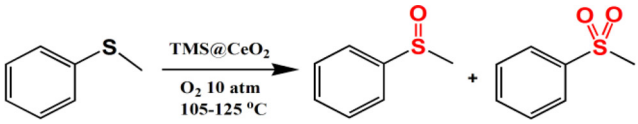

	Catalyst	SSA (m^2/g)	T (°C)	Conv. (%)	SO (%)	SO_2 (%)
1	–	–	105	<0.1	–	–
2	50%$Mn(OAc)_2$@CeO_2	455	105	8.0	80	19
3	CeO_2	192	105	1.1	73	25
4	$Mn(OAc)_2$	–	105	<0.1	–	–
5[b]	50%$Mn(OAc)_2$+50%CeO_2	–	105	0.8	95	–
6[c]	50%$Mn(OAc)_2$@CeO_2-300°C	–	105	1.5	91	5
7	50%$Fe(OAc)_2$@CeO_2	203	105	2.2	81	17
8	50%$Co(OAc)_2$@CeO_2	186	105	0.9	96	–
9	50%$Ni(OAc)_2$@CeO_2	234	105	0.5	95	–
10	50%$Cu(OAc)_2$@CeO_2	196	105	1.1	98	–
11	20%Fe30%$Mn(OAc)_2$@CeO_2	376	105	7.1	73	25
12	20%Cu30%$Mn(OAc)_2$@CeO_2	344	105	4.3	87	11
13	10%$Mn(OAc)_2$@CeO_2	258	105	1.3	75	24
14	20%$Mn(OAc)_2$@CeO_2	257	105	4.7	63	34
15	30%$Mn(OAc)_2$@CeO_2	275	105	5.9	66	32
16	70%$Mn(OAc)_2$@CeO_2	307	105	2.9	95	–
17	50%$Mn(acac)_2$@CeO_2	154	105	2.7	97	–
18	50%$Mn(OAc)_2$@CeO_2	455	115	11.2	84	14
19	50%$Mn(OAc)_2$@CeO_2	455	125	15.4	84	13
20[d]	50%$Mn(OAc)_2$@CeO_2	455	105	25.4	60	37
21[e]	50%$Mn(OAc)_2$@CeO_2	455	105	98.3	44	53
22[f]	50%$Mn(OAc)_2$@CeO_2	455	105	<0.1	–	–
23[g]	50%$Mn(OAc)_2$@CeO_2	455	105	<0.1	–	–

[a] Reaction condition: methyl phenyl sulfide 1 mmol, anisole 1 mmol (internal standard), catalyst 20 mg, CH_3CN 5 mL, O_2 10 bar, 23 h. SO: methyl phenyl sulfoxide, SO_2: methyl phenyl sulfone. [b] A physical mixture with 50 mol% $Mn(OAc)_2$ and 50 mol% CeO_2. [c] 50%$Mn(OAc)_2$@CeO_2 catalyst was treated at 300°C in air for 2 h. [d] Methyl phenyl sulfide 0.2 mmol with 50 mg catalyst in this run. [e] Methyl phenyl sulfide 0.1 mmol with 200 mg catalyst in this run. [f] In argon. [g] 30%H_2O_2 (200 μL) was used in place of O_2.

composed of agglomerated nanoparticles of ~2–5 nm, generating a high degree of interstitial porosity (Figure 3b, 3d). High-resolution STEM-HAADF images together with electron energy loss spectroscopy (EELS) showed the crystalline structure of ceria with TMSs evenly dispersed in the lattice fringes.

Among the selective oxidation processes, catalytic transformation of sulfides into high-value sulfoxides/sulfones is an important process widely investigated for the preparation of numerous chemically, medicinally, and biologically active compounds.[9] Therefore, the oxidation of methyl phenyl sulfide (MPS) was selected as a model reaction to study the catalytic activity of TMS@CeO_2. No products were detected in the blank oxidation of MPS without catalysts (**Entry 1,** Table 1). In the presence of 50%$Mn(OAc)_2$@CeO_2, the oxidation occurred with methyl phenyl sulfoxide (MPSO) as the main product (conv.: 8%, **Entry 2,** Table 1). In contrast, CeO_2 alone afforded only limited activity, and the $Mn(OAc)_2$ salt could not promote this process, suggesting that $Mn(OAc)_2$ doping can significantly enhance the catalytic activity of pristine CeO_2 (**Entries 3–4,** Table 1). A physical mixture of $Mn(OAc)_2$ and CeO_2 was also investigated in the process with relatively low MPS conversion, similar to the performance of CeO_2 alone (**Entry 5,** Table 1). Hence, a molecular- or atomic-scale interaction between Mn $(OAc)_2$ and CeO_2 was found to be necessary for the synergetic activation of O_2. It was observed that the chemical environment of the dopant also played a key role. For example, only 1.5% MPS was converted if the 50%$Mn(OAc)_2$@CeO_2 catalyst was further treated at 300°C for 2 h (**Entry 6,** Table 1). The FTIR study suggests that the acetate anions in 50%$Mn(OAc)_2$@CeO_2 would decompose with the formation of hybrid oxides during 300°C treatment (Figure 1a). Therefore, it is the interfacial interaction between $Mn(OAc)_2$ and CeO_2 that contributes to the activation of O_2 for selective oxidation.

When $Fe(OAc)_2$, $Co(OAc)_2$, $Ni(OAc)_2$, or $Cu(OAc)_2$ salts were doped into CeO_2, no clear enhancement in the catalytic oxidation of MPS was observed. Among the TMSs studied, $Mn(OAc)_2$ afforded the best performance for incorporating with CeO_2 (**Entries 7–10,** Table 1). Ternary catalysts with a third TMS (iron or copper) doping into $Mn(OAc)_2$@CeO_2 were then studied in MPS oxidation. The replacement of partial $Mn(OAc)_2$ by iron or copper salts lowered the catalytic activity of 50%$Mn(OAc)_2$@CeO_2 (**Entries 11–12,** Table 1). Hence, $Mn(OAc)_2$ is an optimal salt for doping into CeO_2.

The effect of the $Mn(OAc)_2$ doping amount (10, 20, 30, 50, and 70%) on CeO_2 was then studied in the oxidation of MPS, and 50%$Mn(OAc)_2$@CeO_2 afforded superior activity (**Entries 2, 13–16,** Table 1). It is supposed that both low and high doping amounts decrease active oxygen species formed at the exact

Table 2. Aerobic and selective oxidation of various sulfides by a 50%$Mn(OAc)_2$@CeO_2 catalyst [a]

	Substrate	Time (h)	Conv. (%)	Product Sel. (%)	Product Sel. (%)
1	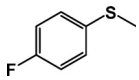	23	81	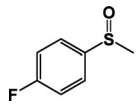 47	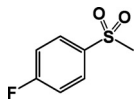 50
2	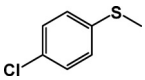	23	85	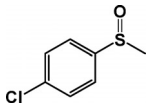 45	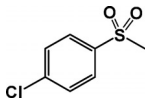 52
3	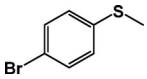	23	91	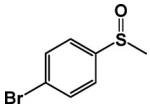 42	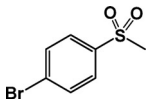 52
4	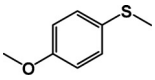	23	> 99	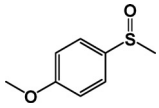 24	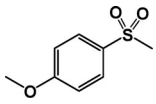 73
5	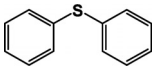	15	> 99	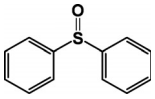 32	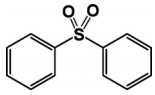 65
6	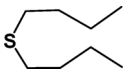	28	42	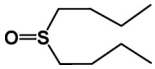 97	

[a] Reaction conditions: sulfide 0.1 mmol, anisole 0.1 mmol (internal standard), 50%$Mn(OAc)_2$@CeO_2 catalyst 200 mg, CH_3CN 5 mL, 105°C, O_2 10 bar.

interface of $Mn(OAc)_2$ and CeO_2; while 50%$Mn(OAc)_2$@CeO_2 affords the maximum active oxygen species. Another manganese salt—$Mn(acac)_2$ can also be doped into CeO_2; and the hybrid material showed a specific surface area of 154 m^2/g. However, the 50%$Mn(acac)_2$@CeO_2 catalyst resulted in only 2.7% MPS conversion (**Entry 17,** Table 1). In comparison with $Mn(OAc)_2$, the bigger molecular size of $Mn(acac)_2$ may influence the approaching of the manganese center into the CeO_2 surface for a synergetic O_2 activation.

Controlled runs with 50%$Mn(OAc)_2$@CeO_2 at different temperatures (105, 115, and 125°C) revealed that the catalytic oxidation was accelerated at a high reaction temperature. The conversion of MPS was enhanced from 8.0 to 15.4% by increasing the temperature from 105 to125°C (**Entries 2, 18–19,** Table 1). After the optimization of catalyst amounts, a high MPS conversion of 98.3% was achieved with both MPS and sulfone as products (**Entries 20–21,** Table 1). Controlled oxidation in argon confirmed that molecular oxygen is the oxidant in the process (**Entry 22,** Table 1). These catalytic results suggested that 50%$Mn(OAc)_2$@CeO_2 is an active catalyst for O_2-based selective oxidation at relative low temperature (105°C).

Next, we explored the general applicability of the $Mn(OAc)_2$@CeO_2 catalyst for the selective oxidation of sulfides. Hydrogen peroxide (H_2O_2) is another useful oxidant with a higher oxidative activity than O_2. When 30%H_2O_2 was used as the oxidant, no any products were observed in 4 h (**Entry 23,** Table 1). A careful observation showed that a number of gas bubbles were released immediately after H_2O_2 was added into the reactants with the catalysts. In the presence of $Mn(OAc)_2$@CeO_2, the H_2O_2 may rapidly decompose into O_2 without the formation of active species attacking the sulfide.[10] Compared with peroxides (e.g., H_2O_2 or tert-butylhydroperoxide), O_2 is much more welcome as an oxidant with respect to abundant availability, low cost, and environmentally friendly character. So it is highly desired that $Mn(OAc)_2$@CeO_2 can activate inert O_2 for selective oxidation.

The transformation of different sulfides was then studied in the presence of $Mn(OAc)_2$@CeO_2/O_2 (Table 2). The $Mn(OAc)_2$@CeO_2 catalyst functioned well in the selective oxidation of MPS-bearing electron-withdrawn groups (e.g. -F, -Cl, or Br) with high conversions (**Entries 1–3,** Table 2). The selective oxidation of 4-methoxythioanisole and diphenyl sulfide proceeded smoothly, and high conversions for both substrates were obtained with $Mn(OAc)_2$@CeO_2 as a catalyst (**Entries 4–5,** Table 2). The electron-donating effect of methoxy- and phenyl- groups may contribute to the O_2 addition into sulfur atoms. $Mn(OAc)_2$@CeO_2 can also promote the selective oxidation of aliphatic sulfide. The dibutyl sulfide oxidation gave a moderate conversion of ~42% with dibutyl sulfoxide as the sole product (**Entry 6,** Table 2).

In addition, the $Mn(OAc)_2$@CeO_2 solid catalyst can be recovered by simple filtration. The liquid phase of the reaction mix-

ture was collected by hot filtration after the MPS oxidation and analyzed by inductively coupled plasma mass spectrometry (ICP-MS). The concentration of manganese ion was 0.27 ppm and the amount of dissolved manganese was very low (0.041 % of the total manganese), suggesting that the $Mn(OAc)_2$ species have been incorporated in the catalyst with strong interaction to ceria. The recycled catalyst can be reused at least six cycles without any significant loss in catalytic activity, arguing for the good stability of $Mn(OAc)_2@CeO_2$ as a catalyst (**Table S1**). So, it is considered that the $Mn(OAc)_2@CeO_2$ catalyst is catalyzing the oxidation in heterogeneous way.

In summary, a series of doped ceria catalysts with TMSs dispersed at atomic scale in the matrix were prepared by a facile IL-assisted co-assembly. The incorporation of TMSs into ceria greatly benefitted the porosity and performance of ceria by, for example, enhancement of the specific surface area from 192 to 455 m^2/g and an eightfold increase in catalytic activity. Under optimized conditions, $Mn(OAc)_2@CeO_2$ enabled the selective and aerobic oxidation of various sulfides to the corresponding sulfoxides/sulfones with moderate to high conversions, where a synergetic interaction between $Mn(OAc)_2$ and CeO_2 was observed. The reactive $Mn(III)(OAc)_2$-oxygen complexes, together with oxygen vacancy–rich CeO_2, are believed to act as active intermediates for O_2 addition into sulfides. Both catalyst reusing and TMS loss measurements confirmed the stability of TMS in the ceria backbone. In some view, current strategy can support soluble TMSs into porous materials as heterogeneous catalysts. All in all, we confirmed the possibility of exploiting ceria-based catalysts for selective oxidation. In this regard, the rich library of ceria-based materials available will provide many potential catalysts for controlled oxidations in both organic synthesis and chemical industry.

Experimental Section, Figure S1-S3 and Table S1 are available in Supporting Information.

Acknowledgment

P. F. Z. and S. D. were supported by the U.S. Department of Energy, Office of Science, Basic Energy Sciences, Chemical Sciences, Geosciences, and Biosciences Division. The electron microscopy at ORNL was supported by the U.S. Department of Energy, Office of Science, Basic Energy Sciences, Materials Sciences and Engineering Division and performed in part as a user project at the ORNL Center for Nanophase Materials Sciences, which is a DOE Office of the Science User Facility.

Keywords: Mesoporous Materials · Ionic Liquids · Oxidation · Ceria Catalyst · Template Synthesis

[1] a) A. Trovarelli, *Catal. Rev.* **1996**, *38*, 439–520; b) Y. Li, Q. Fu, M. Flytzani-Stephanopoulos, *Appl. Catal. B* **2000**, *27*, 179–191; c) S. Scirè, S. Minicò, C. Crisafulli, C. Satriano, A. Pistone, *Appl. Catal. B* **2003**, *40*, 43–49; d) A. Asati, S. Santra, C. Kaittanis, S. Nath, J. Manuel Perez, *Angew. Chem.* **2009**, *121*, 2344–2348; *Angew. Chem. Int. Ed.* **2009**, *48*, 2308–2312; e) C. Xu, X. Qu, *NPG Asia Mater.* **2014**, *6*, 90; f) A. Abad, P. Concepción, A. Corma, H. García, *Angew. Chem.* **2005**, *117*, 4134–4137; *Angew. Chem. Int. Ed.* **2005**, *44*, 4066–4069.

[2] a) Y. Huang, A. Wang, L. Li, X. Wang, D. Su, T. Zhang, *J. Catal.* **2008**, *255*, 144–152; b) J. H. Holles, M. A. Switzer, R. J. Davis, *J. Catal.* **2000**, *190*, 247–260; c) Q. Fu, H. Saltsburg, M. Flytzani-Stephanopoulos, *Science* **2003**, *301*, 935–938; d) X. Tang, Y. Li, X. Huang, Y. Xu, H. Zhu, J. Wang, W. Shen, *Appl. Catal. B* **2006**, *62*, 265–273; e) M. Cargnello, J. J. Delgado Jaén, J. C. Hernández Garrido, K. Bakhmutsky, T. Montini, J. J. Calvino Gámez, R. J. Gorte, P. Fornasiero, *Science* **2012**, *337*, 713–717; f) J. B. Park, J. Graciani, J. Evans, D. Stacchiola, S. Ma, P. Liu, A. Nambu, J. F. Sanzc, J. Hrbeka, J. A. Rodrigueza, *Proc. Natl. Acad. Sci.* USA **2009**, *106*, 4975–4980; g) J. S. Elias, M. Risch, L. Giordano, A. N. Mansour, S. H. Yang, *J. Am. Chem. Soc.* **2014**, *136*, 17193–17200; h) P. Venkataswamy, K. N. Rao, D. Jampaiah, B. M. Reddy, *Appl. Catal. B* **2014**, *162*, 122–132; i) J. Fan, X. Jiang, H. Min, D. Li, X. Ran, L. Zou, Y. Sun, W. Li, J. Yang, W. Teng, G. Li, D. Y. Zhao, *J. Mater. Chem. A* **2014**, *2*, 10654–10661.

[3] a) A. Corma, P. Concepción, M. Boronat, M. J. Sabater, J. Navas, M. J. Yacaman, E. Larios, A. Posadas, M. Arturo López-Quintela, D. Buceta, E. Mendoza, G. Guilera, A. Mayoral, *Nat. Chem.* **2013**, *5*, 775–781; b) T. Punniyamurthy, S. Velusamy, J. Iqbal, *Chem. Rev.* **2005**, *105*, 2329–2363; c) L. Kesavan, R. Tiruvalam, M. H. A. Rahim, M. I. b. Saiman, D. I. Enache, R. L. Jenkins, N. Dimitratos, J. A. Lopez-Sanchez, S. H. Taylor, D. W. Knight, C. J. Kiely, G. J. Hutchings, *Science* **2011**, *331*, 195–199; d) S. Yamazoe, K. Koyasu, T. Tsukuda, *Acc. Chem. Res.* **2014**, *47*, 816.

[4] a) C. T. Campbell, C. H. F. Peden, *Science* **2005**, *309*, 713–714; b) F. Esch, S. Fabris, L. Zhou, T. Montini, C. Africh, P. Fornasiero, G. Comelli, R. Rosei, *Science* **2005**, *309*, 752–755.

[5] a) M. Tamura, K. Tomishige, *Angew. Chem.* **2015**, *127*, 878–881; *Angew. Chem. Int. Ed.* **2015**, *54*, 864–867; b) Y. Wang, F. Wang, Q. Song, Q. Xin, S. Xu, J. Xu, *J. Am. Chem. Soc.* **2013**, *135*, 1506–1515.

[6] a) D. Gu, F, Schüth, *Chem. Soc. Rev.* **2014**, *43*, 313–344; b) R. Ryoo, *Nat. Chem.* **2009**, *1*, 105–106; c) P. D. Yang, D. Y. Zhao, D. I. Margolese, B. F. Chmelka, G. D. Stucky, *Nature* **1998**, *396*, 152–155.

[7] a) V. Molinari, C. Giordano, M. Antonietti, D. Esposito, *J. Am. Chem. Soc.* **2014**, *136*, 1758–1761; b) P. F. Zhang, H. Lu, Y. Zhou, L. Zhang, Z. Wu, S. Yang, H. Shi, Q. Zhu, Y. Chen, S. Dai, *Nat. Commun.* **2015**, *6*, 8446; c) H. Lu, P. F. Zhang, Z.-A. Qiao, J. Zhang, H. Zhu, J. Chen, Y. Chen, S. Dai, *Chem. Commun.* **2015**, *51*, 5910–5913.

[8] P. F. Zhang, Y. Gong, Z. Wei, J. Wang, Z. Zhang, H. Li, S. Dai, Y. Wang, *ACS Appl. Mater. Interfaces* **2014**, *6*, 12515–12522.

[9] a) Y. Imada, H. Iida, S. Ono, S.-I. Murahashi, *J. Am. Chem. Soc.* **2003**, *125*, 2868–2869; b) M. H. V. Huynh, L. M. Witham, J. M. Lasker, M. Wetzler, B. Mort, D. L. Jameson, P. S. White, K. J. Takeuchi, *J. Am. Chem. Soc.* **2003**, *125*, 308–309; c) E. Boring, Y. V. Geletii, C. L. Hill, *J. Am. Chem. Soc.* **2001**, *123*, 1625–1635; d) A. M. Khenkin, G. Leitus, R. Neumann, *J. Am. Chem. Soc.* **2010**, *132*, 11446–11448; f) J. Legros, C. Bolm, *Chem. A Euro. J* **2005**, *11*, 1086–1092; g) P. F. Zhang, Y. Wang, H. R. Li, M. Antonietti, *Green Chem.* **2012**, *14*, 1904–1908; h) F. Bigi, A. Corradini, C. Quarantelli, G. Sartori, *J. Catal.* **2007**, *250*, 222–230.

[10] S. Pati, Z. Rappoport, *The Synthesis of Sulphones, Sulphoxides, and Cyclic Sulphides*, John Wiley and Sons, New York, **1994**.

Submitted: April 11, 2016
Accepted: April 18, 2016